Springer

Journal of Mechanical Science and Technology 22 (2008) 1757~1764

Journal of Mechanical Science and Technology

www.springerlink.com/content/1738-494x
DOI 10.1007/s12206-008-0608-1

A self-sensing technology of active magnetic bearings using a phase modulation algorithm based on a high frequency voltage injection method

Young Ho Park[1], Dong Chul Han[1,*], In Hwang Park[2], Hyeong Joon Ahn[3] and Dong Young Jang[4]

[1]*School of Mechanical & Aerospace Engineering, Seoul National University, Seoul 151-742, Korea*
[2]*BK21 School for Creative Engineering Design of Next Generation Mechanical and Aerospace Systems, Seoul 151-742, Korea*
[3]*Department of Mechanical Engineering, Soongsil University, Seoul 156-743, Korea*
[4]*Industrial & Information Systems Engineering, Seoul National University of Technology, Seoul 139-743, Korea*

(Manuscript Received April 14, 2008; Revised May 13, 2008; Accepted June 9, 2008)

Abstract

Conventional AMB(active magnetic bearings) systems consist of electromagnetic coils, position sensors, power amplifiers and a feedback controller. This hardware configuration can lead to a structural complexity, problems of space limitations for the installation, and position control difficulties due to the non-collocation of actuators and sensors. In this paper, a self-sensing mechanism is proposed to resolve such limitations of the general AMB system. The proposed self-sensing scheme uses a phase difference of the injected current of two opposite electromagnetic actuators while an object is levitating between the actuators. The relationship between the phase difference of injected currents and the position of a levitated object was theoretically derived and linearized. In order to realize the proposed self-sensing scheme, a signal processing algorithm was developed. The frequency response of the estimator was measured to verify the performance of the proposed self-sensing scheme. In addition, a magnetic levitation and a disturbance rejection response were experimentally obtained to verify the feasibility of the proposed self-sensing mechanism. Experimental results showed that the developed self-sensing technique has similar performance as a practical gap sensor.

Keywords: Active magnetic bearing; Self-sensing; Phase modulation; Position sensor; Feedback controller, Pulse width modulation(PWM); Signal processing algorithm; Position estimator

1. Introduction

In recent decades, AMBs have been widely used due to their unique advantages such as non-contact, lubrication-free support and controllability of actuator characteristics in many industrial machines. By virtue of such merits, AMB has become an essential machine element of high-speed rotating machinery, including turbo molecular pumps and high-speed machining centers. The need for AMBs has been also increasing in non-traditional application areas where compact size is required. For example, small-sized AMBs can be applied to portable hard disk drive systems, artificial heart blood pumps and audio loudspeakers.

Conventional AMB systems typically consist of a pair of electromagnetic coils acting as actuators, position sensors, power amplifiers and a feedback controller. This hardware configuration can lead to a structural complexity and problems of space limitations for the installation. In addition, the non-collocation of actuators and sensors may cause difficulties in position control algorithms. If the electromagnetic coils can serve as a position sensor as well as an actuator, the above problems can be easily solved. This kind of sensing mechanism is termed 'self-sensing' mechanism where the levitated object position is indirectly measured via the currents flowing in the coils. Since

*Corresponding author. Tel.: +82 2 880 7139, Fax.: +82 2 883 1513
E-mail address: dchan@snu.ac.kr

the variation of the air gap between the electromagnets and the levitated object results in inductance changes, the air gap can be modeled as an inductor. If the inductance can be estimated by the currents, the object position information can be obtained by the currents.

There have been two approaches to realize the self-sensing technology for AMB systems. One is to use a state model. In this approach, the object position can be estimated by constructing state observer and measuring the electromagnetic coil current. This was first studied by Visher et al. [1]. However, due to poor observability at high frequency [2], detailed modeling and considerations for changes of environments are necessary. The other approach is to use a high frequency carrier using PWM (pulse width modulation) power amplifiers which drive the electromagnetic coils. Since the current ripples generated by PWM carrier component are related to inductance variation, the object position can be estimated by measuring the high frequency current ripple. This was suggested by Okada et al. [3]. However, since the current ripples corresponding to PWM carrier frequency may also be changed by duty ratio, it is necessary to take the duty ratio into the consideration for the controller design by measuring voltage ripples [4, 5] or using a nonlinear observer [6, 7, 8]. For improved position accuracy, magnetic material permeability can be compensated by using an approximated static permeability curve [9, 10].

Although several self-sensing technologies have been proposed for years, applying such technologies for industrial applications still remains a challenging problem. To improve the performance of conventional self-sensing technologies and to make the technology more applicable to industrial applications, a self-sensing scheme using a phase modulation algorithm based on a high frequency voltage injection method is proposed. Unlike the other self-sensing technologies, the proposed technology does not need any compensations including duty ratio. In addition, since white noises generally do not have a phase information but an amplitude information, the proposed method may be robust to noise over other technologies.

This paper will begin with a theory of the proposed self-sensing mechanism, followed by a signal processing algorithm for the self-sensing scheme (section 2.2). Compensation methods for the proposed theory for improving the accuracy of the AMB system is described in section 3.1. Finally, frequency response of the proposed estimation algorithm is experimentally measured to evaluate the dynamic performance. The self-sensing signal is compared to a reference eddy current sensor signal when a one degree-of-freedom mechanical system is magnetically levitated and disturbance is rejected (section 3.2).

2. Proposed self-sensing scheme

2.1 Design

Fig. 1(a) shows the proposed self-sensing AMB system scheme. This system is composed of a pair of electromagnetic actuators (EMA1 and EMA2), PWM power amplifiers, current controllers, a position controller and a position estimator. A conventional AMB system as shown in Fig. 1(b) has a position sensor (e.g., eddy-current, inductive or capacitive position sensor) which causes hardware complexity and installation problem. But the proposed system uses the position estimator instead of a position sensor. This scheme can resolve the limitation caused by a posi-

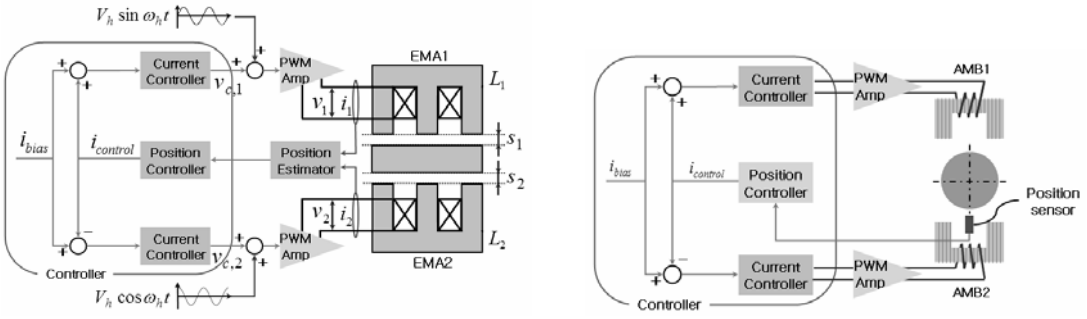

(a) The proposed AMB system

(b) A conventional AMB system

Fig. 1. The proposed and a conventional AMB systems.

tion sensor of the conventional AMB system.

The object moves along the s_1 or s_2 direction. The electromagnetic actuator in Fig. 1(a) is electrically modeled as shown in Fig. 2.

In Fig. 2, since the core loss R_E and the coil capacitance C_P can be negligible, the voltage v and the current i of the EMA have the following relationship.

$$v = R \cdot i + L\frac{di}{dt} \tag{1}$$

In addition to the voltage signals v_{c1}, v_{c2} to control the EMA currents, the high-frequency sinusoidal waveforms $V_h \sin\omega_h t$, $V_h \cos\omega_h t$ for self-sensing estimation are applied to the EMAs as shown in Fig. 1(a). If the injection frequency ω_h is much higher than the frequency bandwidth to control the EMA currents, the ω_h components in Eq. (1) can be considered alone. Then, the amplitude and the phase of the EMA currents corresponding to ω_h can be obtained as given in Eq. (2). For simplicity, the EMA1 where the sine waveform is injected is considered only in Fig. 2.

$$i = I_h \sin(\omega_h t + \phi) \tag{2}$$

where $I_h = \dfrac{V_h}{\sqrt{R^2 + (\omega_h L)^2}}, \tan\phi = -\dfrac{\omega_h L}{R}$

The inductance L of the EMA is a function of coil turn number n, cross-sectional area A of magnetic flux passage, magnetic permeability μ_0 in vacuum, and gap distance s between the EMA and the levitated object [11].

$$L = \frac{\mu_0 n^2 A}{2s} \tag{3}$$

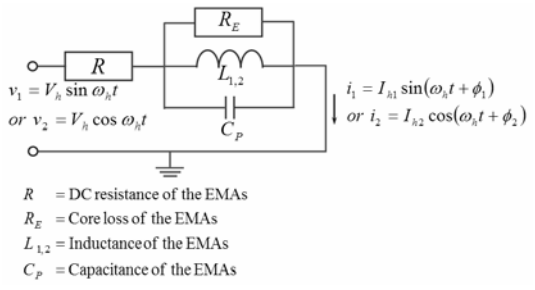

Fig. 2. Electrical model for the electromagnetic actuators.

From Eqs. (2) and (3), the change in the gap distance causes the change in the inductance, resulting in the change of EMA current amplitude and phase. In this paper, the change of the EMA current phase will be used to estimate the change of the gap distance. Since the relationship between ϕ and s in Eqs. (2) and (3) is nonlinear, it is difficult to implement ϕ - s relationship while applying a position control algorithm. Thus, the ϕ - s relationship needs linearization at operating points. For linearization, it is assumed that the moving distance of the levitated object is very small from the operating point. Then, s, L and ϕ can be expressed as following.

$$s = s_0 + \Delta s \tag{4}$$

$$L = L_0 + \Delta L \tag{5}$$

$$\phi = \phi_0 + \Delta\phi \tag{6}$$

where subscripts 0 and Δ denote the operating point and small deviations, respectively.

To linearize $\Delta\phi - \Delta s$ relationship, $\Delta L - \Delta s$ and $\Delta\phi - \Delta L$ linear relationships are utilized because t he $\Delta\phi - \Delta s$ linear relationship cannot be obtained directly.

Substituting s in Eq. (4) into s in Eq. (3) and using the Taylor series expansion at s_0, the resulting inductance L is modified as following.

$$\begin{aligned} L &= \frac{\mu_0 n^2 A}{2}\left(\frac{1}{s_0 + \Delta s}\right) \\ &\approx \frac{\mu_0 n^2 A}{2s_0}\left(1 - \frac{\Delta s}{s_0}\right) \\ &= L_0\left(1 - \frac{\Delta s}{s_0}\right) \end{aligned} \tag{7}$$

where $L_0 = \dfrac{\mu_0 n^2 A}{2s_0}$.

Comparing the Eqs. (5) and (7), ΔL is expressed as follows.

$$\Delta L = -\frac{L_0}{s_0}\Delta s \tag{8}$$

So, the linear relationship between ΔL and Δs is acquired as shown in Eq. (8).

Now, to get $\Delta\phi - \Delta L$ linear relationship, let us substitute ϕ in Eq. (6) into ϕ in Eq. (2). Then we can obtain,

$$\begin{aligned}\tan\phi &= \tan(\phi_0 + \Delta\phi) \\ &= -\frac{\omega_h \cdot (L_0 + \Delta L)}{R} \\ &= \tan\phi_0 - \frac{\omega_h \cdot \Delta L}{R}\end{aligned} \tag{9}$$

where $\tan\phi_0 = -\frac{\omega_h \cdot L_0}{R}$.

On the other hand, $\tan\phi$ in Eq. (2) can be rewritten by using the Taylor series expansion at ϕ_0.

$$\tan\phi = \tan\phi_0 + \Delta\phi \sec^2\phi_0 \tag{10}$$

Comparing the Eqs. (9) and (10), $\Delta\phi - \Delta L$ relationship can be obtained.

$$\begin{aligned}\Delta\phi &= -\frac{1}{\sec^2\phi_0} \cdot \frac{\omega_h \cdot \Delta L}{R} \\ &= -\frac{\omega_h R}{R^2 + (\omega_h L_0)^2} \Delta L\end{aligned} \tag{11}$$

where $\sec\phi_0 = \sqrt{R^2 + (\omega_h \cdot L_0)^2} / R$.

Consequently, the $\Delta s - \Delta\phi$ linear relationship is obtained from Eqs. (8) and (11) as given in Eq. (12).

$$\Delta s = \frac{s_0 \omega_h L_0}{R} \Delta\phi; \quad (\omega_h \cdot L_0 >> R) \tag{12}$$

Since the position change Δs is linearly dependent on the phase change $\Delta\phi$, the position s can be estimated by measuring the coil current phase change $\Delta\phi$, multiplying $\Delta\phi$ by $\frac{s_0 \omega_h L_0}{R}$ which is constant under a specific system and adding the operating position s_0.

2.2 Signal processing algorithm

In general, conventional EMAs can be controlled by feedback of the opposite position difference $s_1 - s_2$, shown in Fig. 1(a). However, as stated in Eq. (12), the proposed self-sensing EMAs can be controlled by the current phase difference $\phi_1 - \phi_2$ instead of the position difference $s_1 - s_2$. In order to get the phase difference, a trigonometric conversion formula that converts multiplication into sum is used. When the trigonometric conversion formula is used, the phase difference of injection signals should be $\pi/2$. This is because the phase difference of two injection signals can be approximately acquired by using the sinusoidal functions. For instance, when multiplication of two sinusoidal functions with same phase is converted into sum by using the trigonometric conversion formula, it is expressed by the sum of two cosine functions. Therefore, if the phase difference of two injection signals is very small, the corresponding cosine value of the phase difference is nearly 0; hence, the phase difference cannot be obtained approximately. On the other hand, when multiplication of two sinusoidal functions with $\pi/2$ phase difference is converted into sum, it is expressed by the sum of two sine functions. Therefore, with the small phase difference, the corresponding sine value of the phase difference can be approximated to the value of phase difference.

From Eq. (2), The currents of two EMAs can be expressed as follows if $\omega_h \cdot L >> R$.

$$i_1 = \frac{V_h}{\omega_h L_1} \sin(\omega_h t + \phi_1) \tag{13}$$

$$i_2 = \frac{V_h}{\omega_h L_2} \cos(\omega_h t + \phi_2) \tag{14}$$

Then the multiplication of the currents can be written as,

$$i_1 i_2 = \frac{V_h^2}{2\omega_h^2 L_1 L_2} \{\sin(2\omega_h t + \phi_1 + \phi_2) + \sin(\phi_1 - \phi_2)\} \tag{15}$$

To remove a doubled high frequency term, a low-pass filter is adopted. Thus the multiplication of the two currents after the low-pass filter can be obtained approximately as follows:

$$LPF(i_1 i_2) \approx \frac{1}{2}\left(\frac{V_h}{\omega_h L_0}\right)^2 (\phi_1 - \phi_2) \tag{16}$$

Since $\sin(\phi_1 - \phi_2) \approx \phi_1 - \phi_2$ and $L_1 L_2 = (L_0^2 - \Delta L^2) \approx L_0^2$ at the operating point, the resulting position difference is estimated by substituting the phase difference in Eq. (16) into Eq. (12). Consequently, we can obtain the final relationship between the phase difference of the injected currents and the position difference of the 2 EMAs as the following.

$$\frac{1}{2}(s_1 - s_2) = \frac{s_0 \omega_h^3 L_0^3}{R V_h^2} \cdot LPF(i_1 i_2) \tag{17}$$

Fig. 3 shows the signal processing block diagram.

In this diagram, two EMAs currents are multiplied by each other, filtered by LPF and amplified. Finally, the intended position difference $(s_1 - s_2)/2$ is obtained.

3. Experiments

3.1 Compensation of the theoretical inductance

Since the proposed self-sensing algorithm is linearized at the operating point, the error caused by non-linearity is augmented by increasing the deviation distance from the operating point. In order to compensate for the error, the inductances of the EMAs are measured with a conventional LCR meter (FLUKE Inc., PM6306). Fig. 4 shows the result of the inductance value of the EMA measured with LCR meter compared to the theoretical result in Eq. (8). As shown in Fig. 4, the inductance value measured with LCR meter is smaller than the theoretical value.

Since it is difficult to theoretically develop the cause of the difference between the two results, a modification constant K was introduced. The modification constant K of 20.5 was experimentally found. Then the modification of ΔL in Eq. (8) and Δs in Eq. (12) can be performed as follows.

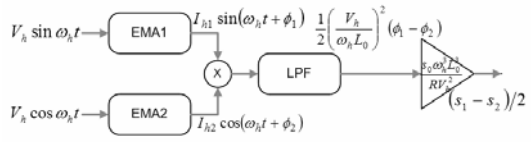

Fig. 3. Signal processing block diagram.

$$\Delta L = -\frac{1}{K}\frac{L_0}{s_0}\Delta s \tag{18}$$

$$\Delta s = K \frac{s_0 \omega_h L_0}{R} \Delta \phi \tag{19}$$

Using Eq. (19) and the experimentally obtained modification constant K, the experimental result of $\Delta\phi - \Delta s$ relationship is compared to theory as shown in Fig. 5.

The curves in Fig. 5 show that the compensated theoretical curve is almost identical to the measured over the whole operating range except at both ends. The difference at both ends is probably due to ΔL^2 which was neglected from the assumption of $L_1 L_2 = (L_0^2 - \Delta L^2) \approx L_0^2$ in Eq. (17). Since $\Delta L^2 / L_0^2$ is below 0.01 in this system, this error has little effect on the whole AMB system performance.

3.2 Experimental results

The frequency response of the position estimator is necessary to verify the performance of the proposed self-sensing technology. A test rig was designed and constructed to get the frequency response as shown in Fig. 6. This test rig is composed of a cantilever, two EMAs and two conventional eddy-current gap sensors. The cantilever was installed at the center between two EMAs. The gap sensors were installed as close as possible to the EMAs. The EMAs were controlled with a digital signal processor (TI Inc., TMS320F2812) and PWM power amplifiers were made with smart power module (Fairchild Inc., FSAM10SH60A). The reference gap sensor was an eddy-current sensor (KAMAN Inc., KD23001SUM). Table 1 shows the specifications of EMAs.

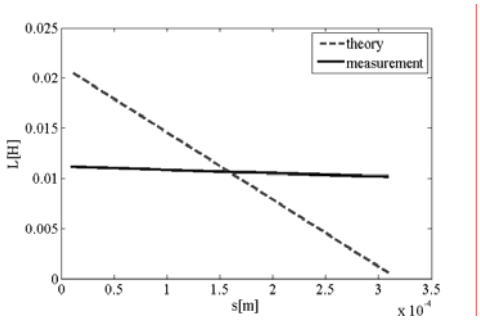

Fig. 4. Comparison of measured EMA inductance value to theoretical value at 3kHz.

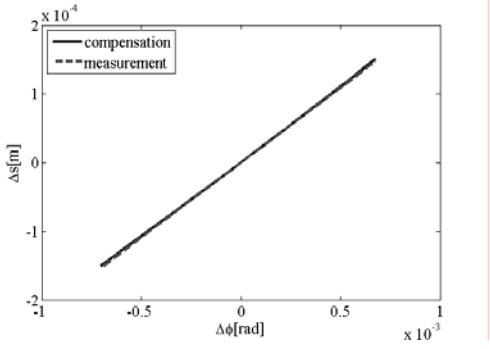

Fig. 5. EMA current phase change vs object position change after compensation.

Table 1. EMA specifications.

Nominal air gap	0.3mm
Number of turns of each coil	152
Cross sectional area of air gap	166.6mm^2
Nominal inductance	0.0136H
Resistance	1.5Ω
Switching frequency	12kHz
Injection frequency	3.0kHz
Magnitude of injection voltage	10V
DC link voltage	45V

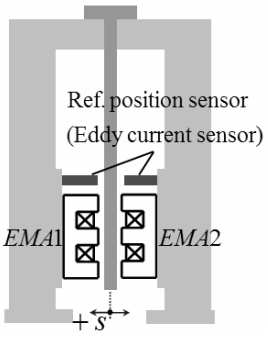

(a) The model of test rig

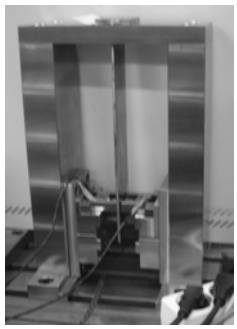

(b) The real image of test rig

Fig. 6. Cantilever test rig for EMA performance.

The frequency response of position estimator was measured as follows.

1) The cantilever was excited by two EMAs where the chirp signal generated by a dynamic signal analyzer (HP Inc., 25670A) was injected.

2) The output signals of the gap sensor and the position estimator were measured.

3) Consequently, the frequency response of the estimator was measured by the ratio of output signal of gap sensor to that of estimator.

Fig. 7 shows the frequency response of the estimator showing bandwidth of about 50Hz. A. Schammass [9, 10] suggested that the compensation of magnetic permeability effect should be considered to improve the self-sensing performance.

To verify the feasibility of the proposed self-sensing mechanism, a one degree-of-freedom mechanical system was designed. As shown in Fig. 8, a mass center of a rolling mass was on a pivot point so that the rolling mass can only rotate around its center of mass. The EMAs are installed at both ends of the rolling mass to control the rotating motion of the rolling mass. Practical gap sensors (KAMAN Inc., KD23001SUM) were installed as close as possible to the EMAs. The controller and power amplifiers were the same as those used previously in the cantilever test rig. The current controller uses a PI control algorithm to control the EMA currents with 300Hz cutoff frequency and the position controller uses a PD control algorithm to control the rolling mass position.

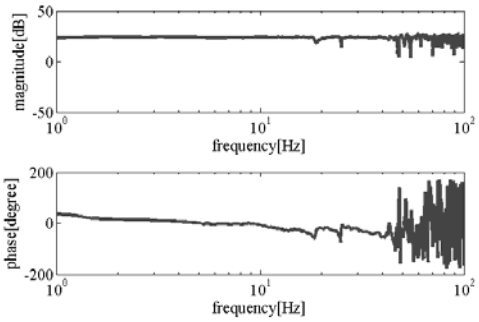

Fig. 7. Frequency response of the position estimator.

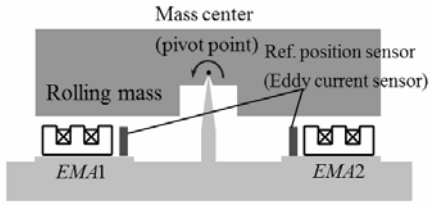

(a) The model of One D.O.F. mechanical system

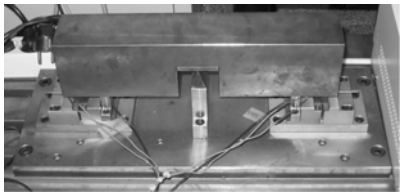

(b) The real image of One D.O.F. mechanical system

Fig. 8. One D.O.F. mechanical system for feasibility test of the proposed self-sensing theory.

Figs. 9 and 10 show a magnetic levitation and a disturbance rejection response, respectively. It can be seen that the levitated object was stably suspended and the disturbance was rejected. These results also show that the self-sensing signal is consistent with the signal from the gap sensor signal. Therefore, it is confirmed that the proposed self-sensing mechanism can be used to both estimate the position of an object and to control the object suspension. As a result, the removal of a position sensor will decrease structural complexity and installation space.

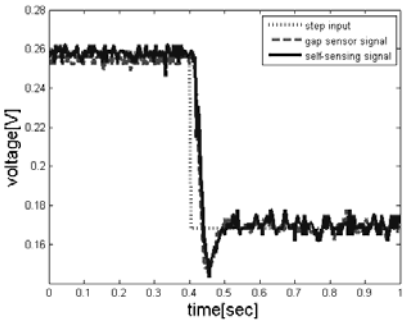

Fig. 9. Magnetic levitation response.

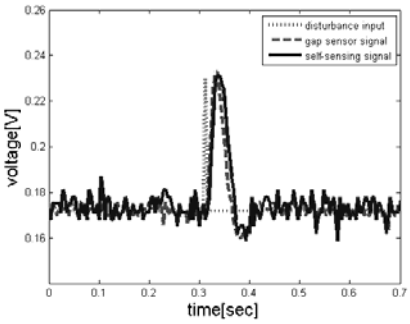

Fig. 10. Disturbance rejection response.

4. Conclusions

This paper proposes a developed self-sensing technology to make it more practicable. The proposed mechanism using the phase modulation algorithm is based on the high frequency voltage injection method with a PWM power amplifier. And the position estimator worked without any compensation about duty ratio changes.

The relationship between the phase change and the levitated object position was theoretically derived and linearized to implement easily. And this relationship was compensated after measured EMA inductance value with LCR meter had been compared to theoretical value. As a result, the modification constant K was discovered experimentally. To realize the phase modulation algorithm a signal processing method was developed by using a trigonometric conversion formula.

To verify the performance of the proposed self-sensing technology, the frequency response of the position estimator was measured through the cantilever test rig. The estimator showed a bandwidth of about 50Hz.

Finally, to verify the feasibility, the magnetic levitation and the disturbance rejection response were obtained through a one degree-of-freedom mechanical system. The results demonstrate that the proposed self-sensing technology shows the same performance as a practical position sensor.

Acknowledgments

This work was supported by the second stage of the Brain Korea 21 Project in 2007 and Ministry of Science & Technology and special thanks are given to the Institute of Advanced Machinery and Design at Seoul National University for a partial support.

Nomenclature

A	: Cross-sectional area of magnetic flux passage
C_P	: Coil capacitance
I_h	: Magnitude of injected current
i	: Current flowing in EMA
i_1, i_2	: Current flowing in EMA1 or EMA2
K	: Modification constant
L	: Inductance of EMA
L_1, L_2	: Inductance of EMA1 or EMA2
L_0	: Inductance at operating point
ΔL	: Small inductance from operating point
n	: Coil turn number
R	: Resistance of EMA
R_E	: Core loss of EMA
s	: Object position from EMA
s_1, s_2	: Object position from EMA1 or EMA2
s_0	: Object position at operating point
Δs	: Small object position from operating point
V_h	: Magnitude of injected voltage
v	: Voltage of EMA
v_1, v_2	: Voltage of EMA1 or EMA2
v_{c1}, v_{c2}	: Control voltage of EMA1 or EMA2
μ_0	: Magnetic permeability in vacuum
ϕ	: Phase of EMA
ϕ_1, ϕ_2	: Phase of EMA1 or EMA2
ϕ_0	: Phase at operating point
$\Delta\phi$	: Small phase from operating point
ω_h	: Frequency of injected signal

References

[1] D. Vischer, Sensorlose und spannungsgesteuerte magnetlager, Ph.D. dissertation, Dept. Mech. Eng., Swiss Federal Inst. Technol., (1988) no. 8665.

[2] L. Kuˇcera, Robustness of self-sensing magnetic bearings, in Proc. Magnetic Bearings Industrial Conf., (1997) 261-270.

[3] Y. Okada, K. Matsuda and B. Nagai, Sensorless magnetic levitation control by measuring the PWM carrier frequency component, in Proc. 3rd Int. Symp. Magnetic Bearings, (1992) 176-183.

[4] V. Iannello, Sensorless Position for an Active Magnetic Bearing. U. S. Patent 5 696 412, (1997).

[5] N. Skricka and R. Markert, Compensation of disturbances on self-sensing magnetic bearings caused by saturation and coordinate coupling, in Proc. 7th Int. Symp. Magnetic Bearings. (2000) 165-170.

[6] M. D. Noh and E. H. Maslen, Position estimation in magnetic bearings using inductance measurements, in Proc. Magnetic Bearings Industrial Conf., (1995) 249-256.

[7] D. T. Montie and E. H. Maslen, Experimental self-sensing results for a magnetic bearing, in Proc. 7th Int. Symp. Magnetic Bearings. (2000) 171-176.

[8] K. S. Peterson, R. H. Middleton and J. S. Freudenberg, Fundamental Limitations in Self-Sensing Magnetic Bearings when Modeled as Linear Periodic Systems, Proceedings of the 2006 American Control Conference Minneapolis, Minnesota, USA, June 14-16, (2006) 4552-4557.

[9] A. Schammass, A self-sensing active magnetic bearing: Modulation approach, Ph.D. dissertation, EPF, Lausanne, (2003) no. 2841.

[10] A. Schammass, R. Herzog, P. Bühler and H. Bleuler, New Results for Self-Sensing Active Magnetic Bearings Using Modulation Approach, IEEE Transactions on Control Systems Technology, 13, no. 4, july (2005) 509-516.

[11] G. Schweitzer, H. Bleuler and A. Traxler, Active Magnetic Bearings: Basics, Properties and Applications of Active Magnetic Bearings, vdf Houchschulverlag AG der ETH Zurich, (1994).